Available online at www.sciencedirect.com
ScienceDirect
Journal of the European Ceramic Society 29 (2009) 2053–2060
www.elsevier.com/locate/jeurceramsoc

$MoSi_2$–Si_3N_4 composites: Influence of starting materials and fabrication route on electrical and mechanical properties

Kh.V. Manukyan [a,b,*], S.L. Kharatyan [a,b], G. Blugan [c], P. Kocher [d], J. Kuebler [c]

[a] *Department of Inorganic Chemistry, Yerevan State University, A. Manukyan 1, Yerevan, AM-0025, Armenia*
[b] *Laboratory of Kinetics of SHS Processes, A.B. Nalbandyan Institute of Chemical Physics NAS of Armenia, P. Sevak 5/2, Yerevan, AM-0014, Armenia*
[c] *Laboratory for High Performance Ceramics, Empa, Swiss Federal Laboratories for Materials Testing and Research, Ueberlandstrasse 129, Duebendorf, CH-8600, Switzerland*
[d] *Institute of Nonmetallic Inorganic Materials, Department of Materials, Swiss Federal Institute of Technology, ETH Zurich, Wolfgang-Pauli-Str. 10, Zurich, CH-8093, Switzerland*

Received 16 April 2008; received in revised form 28 November 2008; accepted 5 December 2008

Abstract

The fabrication method and the mechanical and electrical properties of different $MoSi_2$–Si_3N_4 composite materials were investigated. Commercially available individual compounds, one-stage combustion synthesized $MoSi_2$–Si_3N_4 and submicron $MoSi_2$ powders were used as starting materials, followed by hot pressing. It was found that the sintering atmosphere used, nitrogen or argon, had a significant effect on the phase composition, mechanical and electrical properties of the final materials. It was shown that in some cases partial nitridation of $MoSi_2$ occurred with the formation of $MoSi_2$–Mo_5Si_3–Si_3N_4 ternary composites. The electrical conductivity of the composites depends also on the microstructure of materials. It was shown that the composites fabricated using combustion synthesized $MoSi_2$ powders (500 nm) are characterized by higher flexural strength at room temperature compared to those from commercial powders. On the other hand, the composites fabricated from the commercial powders had higher strength and fracture toughness at elevated temperatures (up to 1200 °C). For all composites, the strength decreased significantly at temperatures over 1000 °C due to the brittle–ductile transition of the $MoSi_2$ phase.

Keywords: Hot pressing; Composites; Electrical properties; Strength; Fracture

1. Introduction

Si_3N_4-based ceramics are among the most important materials for high temperature structural applications, because of their superior properties such as strength, hardness, thermal and chemical stability. The need for improving fracture toughness, high temperature and electrical properties, and machinability of Si_3N_4-based materials has led to the recent development of $MoSi_2$-particle reinforced-Si_3N_4 composites.[1–14] The combination of Si_3N_4 and $MoSi_2$ gives $MoSi_2$–Si_3N_4 composite materials with desirable mechanical properties and good electrical conductivity. The intermetallic compound $MoSi_2$ has long been known as a high temperature material that has excellent oxidation resistance and electrical conductivity ($2 \times 10^5\ \Omega^{-1}\ cm^{-1}$ at room temperature). Also its low cost, high melting point (2020 °C), relatively low density ($6.2\ g\ cm^{-3}$), and ease of machining, make it an attractive structural material.[15,16] However, the poor toughness and low creep resistance that $MoSi_2$ exhibits at ambient and elevated temperature[16,17] limits its application at present.

It was shown that the mechanical behaviour of $MoSi_2$ reinforced-Si_3N_4 matrix composites are influenced by the $MoSi_2$ phase content and $MoSi_2$ phase size.[5] Coarse-phase $MoSi_2$–Si_3N_4 composites exhibited higher room temperature fracture toughness than fine-phase composites, reaching values >8 MPa $m^{1/2}$. On the other hand, the inclusion of a certain amount of electroconductive $MoSi_2$ particles into the insulating Si_3N_4 matrix, similar to the inclusion of TiN particles,[18] can lead to electrically conductive composites and this can facilitate their machining into complex shapes by the economical electrical discharge machining (EDM) technique. $MoSi_2$–Si_3N_4

* Corresponding author at: Department of Inorganic Chemistry, Yerevan State University, A. Manukyan 1, Yerevan, AM-0025, Armenia. Tel.: +374 10 281610; fax: +374 10 281634.
E-mail address: khachat@ichph.sci.am (Kh.V. Manukyan).

0955-2219/$ – see front matter © 2008 Elsevier Ltd. All rights reserved.
doi:10.1016/j.jeurceramsoc.2008.12.015

composites have great potential for high temperature electrical applications. However, only limited data on the electrical conductivity of $MoSi_2$–Si_3N_4 composites dependence on grain size of conductive phase is available in the literature.[8,13]

In the present study the fabrication, mechanical and electrical properties of $MoSi_2$–Si_3N_4 composite materials were investigated. Commercially available individual compounds, one-stage combustion synthesized $MoSi_2$–Si_3N_4 and different $MoSi_2$ powders were used as starting materials. The influence of sintering atmosphere on the phase composition and microstructure of the final materials and their subsequent effect on the high temperature electrical and mechanical properties of dense materials was studied.

2. Experimental

$MoSi_2$–Si_3N_4 composite materials containing 22–40 vol.% $MoSi_2$ were fabricated from the commercial Si_3N_4 (grade M11, H.C. Starck, Germany) and $MoSi_2$ (grade C, H.C. Starck, Germany), as well as salt-assisted combustion synthesized $MoSi_2$ and $MoSi_2$–Si_3N_4 composite powders (synthesis conditions of these two powders are described elsewhere).[19] According to scanning electron microscopy (SEM) analysis the particle size of the combustion synthesized $MoSi_2$ powder was 0.5 μm (Fig. 1a). It also contains a small amount (3–4 wt.%) of Mo_5Si_3. The silicon and iron impurities in it are about 0.7 and 0.1 wt.%, respectively. The average particle size of combustion synthesized $MoSi_2$–Si_3N_4 composite powder is between 1 and 2 μm as shown in Fig. 1b. The main impurities detected in the $MoSi_2$–Si_3N_4 composite powder were silicon (0.7 wt.%) and iron (0.3–0.4 wt.%).

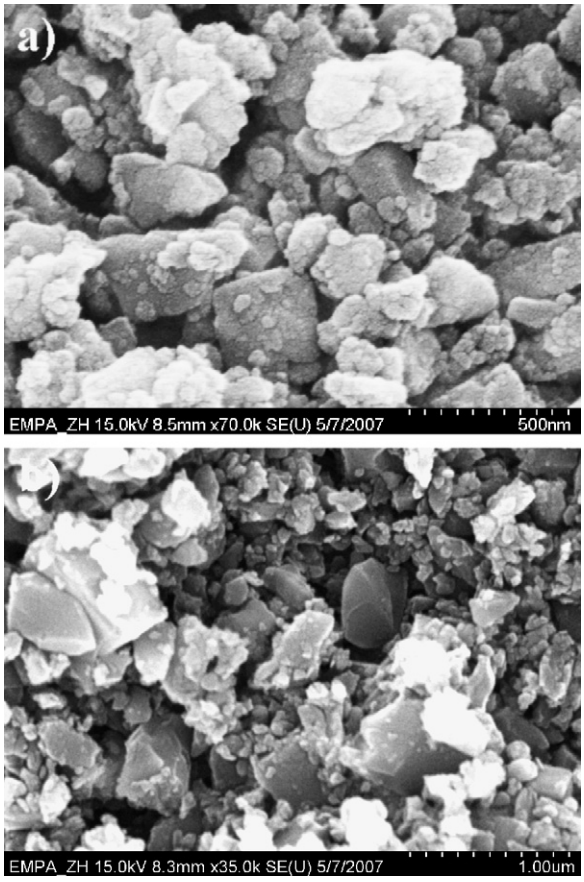

Fig. 1. Microstructure of combustion synthesized $MoSi_2$ (a) and $MoSi_2$–Si_3N_4 composite (b) powders.

The fabrication routes of materials designated as SM1–SM6 are presented in Table 1. Commercial Si_3N_4 and commercial $MoSi_2$ powders were used for fabricating SM2 and SM3 composites. In-house made "*in situ*" synthesized $MoSi_2$–Si_3N_4 composite (containing 22 vol.% of $MoSi_2$) powder was used for fabricating SM1 and SM4 materials. In preparation of SM4, SM5 and SM6 composite materials combustion synthesized $MoSi_2$ powder was used. In all six composites 1.5 vol.% of Al_2O_3 (CT3000 SG, Bassermann Minerals, Germany) and 3.5 vol.% Y_2O_3 (grade C, H.C. Starck, Germany) were used as sintering aids. The starting powders were mixed in isopropanol for 3–4 h by a planetary mill (PM400, Rentsch). Additionally 1 wt.% polyvinyl butyral (PVB) (Mowital B 20H, Clariant GmbH, Germany) was added as a binder to the slurry after the milling process. The slurries were then dried in a rotary evaporator and the powder passed through a 125 μm sieve. The precursor powder mixtures were compacted by uniaxial pressing to produce disc-shaped green bodies 20 and 50 mm in diameter. The powder compacts were hot pressed in BN-coated graphite dies (hot press: *Thermal Technology Inc.*, *Model 383–40*, *modified*) at 30 MPa in 0.1 MPa nitrogen or argon atmosphere at temperatures up to 1700 °C. All six materials (SM1–SM6) were sintered in nitrogen. In argon atmosphere only SM5 and SM6 materials were hot pressed. The hot pressed samples were produced in a disc shape with a diameter of 20 and 50 mm and a thickness of 5–7 mm. Bend-bar specimens with dimensions 3 mm × 4 mm × 45 mm were cut from the sintered materials by conventional diamond machining, and the edges

Table 1
Fabrication route and designations of the composite materials.

Number	Fabrication route	$MoSi_2$ content (vol.%)	Composite designation	Density (%)	
				In nitrogen	In argon
1	Combustion synthesized composite	22	SM1	98.5	–
2	Mixing of commercial $MoSi_2$ and commercial Si_3N_4	30	SM2	99.4	–
3	Mixing of commercial $MoSi_2$ and commercial Si_3N_4	40	SM3	99.7	–
4	SM1 + SHS-$MoSi_2$	30	SM4	98.8	–
5	Mixing of SHS-$MoSi_2$ with commercial Si_3N_4	30	SM5	99.0	99.5
6	Mixing of SHS-$MoSi_2$ with commercial Si_3N_4	40	SM6	99.3	99.6

of the bend bars were chamfered according to the CEN 843-1 standard.[20]

Specimens were then polished and plasma etched for the microstructural analysis using scanning electron microscopy (VEGA TS 5136 Tescan, CZ). Phase composition of sintered materials was determined by X-ray analysis with CuKα radiation on a diffractometer (PANalytical PW 3040/6092 X'Pert PRO). The evaluation of the mechanical properties (fracture toughness and flexural strength) was conducted using four-point bending method using bend-bar specimens with a 40/20 mm load geometry. The fracture toughness, K_{Ic}, of composites was measured at room and elevated temperatures using the single-edge-V-notch beam (SEVNB) method as described in the CEN/TS 14425-5 standard.[21] A notch was cut in the 3 mm side of the bend bar using a specially constructed notching machine and the final notching was performed using a steel razor blade with 1 μm diamond paste. At each testing temperature, two notched specimens for each composition were fractured at a crosshead displacement speed of 0.3 mm min^{-1} (Zwick Z005, Germany). The flexural strength was also measured at room and elevated temperatures using a crosshead displacement speed of 0.5 mm min^{-1} (Zwick 1478, Germany), 3–4 specimens were tested at each temperature. The high temperature electrical conductivity of the composites was measured using the four-probe method in accordance with ASTM standard F43-93.[22] The measurements were carried out at up to 1100 °C in air with a heating rate of 5 °C min^{-1} in an electrical resistance furnace (FHT 1750, Ceram-Aix, Germany).

3. Results and discussions

3.1. Phase composition and microstructure

The composite materials fabricated from the different powders were consolidated by hot pressing in argon or nitrogen atmosphere. After the hot pressing, the surfaces of the sintered discs were cleaned of excess BN by diamond grinding. The density of the sintered materials, measured by water displacement technique, was found to be between 98.5 and 99.7% of the theoretical density (Table 1). Density was calculated from the starting compositions using the rule of mixtures. Grain size and phase composition of the materials are summarized in Table 2. The results of XRD analyses (Fig. 2 and Table 2) indicate that the sintering atmosphere has a significant influence on the final phase composition of the materials. The compacts consolidated in argon atmosphere contained $MoSi_2$ and β-Si_3N_4 (Fig. 2a). However, when nitrogen was used as a sintering atmosphere, partial nitriding of $MoSi_2$ took place by the following reaction:

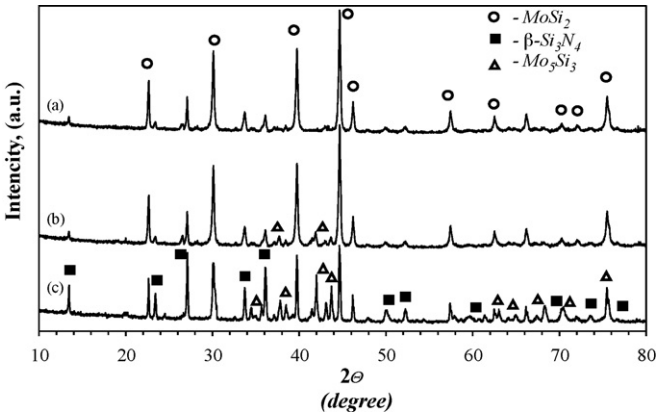

Fig. 2. XRD patterns of the SM5 composite hot pressed in argon (a) and nitrogen (c) and SM4 composite sintered in nitrogen atmosphere (b).

$$15MoSi_2 + 14N_2 \rightarrow 7Si_3N_4 + 3Mo_5Si_3 \quad (1)$$

It can be seen from Fig. 2b that the SM4 composite sintered in nitrogen resulted in the formation of dense material containing $MoSi_2$, β-Si_3N_4 and only small amounts of Mo_5Si_3, while in the case of the SM5 composite (Fig. 2c) significant amounts of initial $MoSi_2$ was nitrided according to reaction (1). It has been reported[2] that Si_3N_4 and $MoSi_2$ phases are thermodynamically stable during the hot pressing at 1650 °C and low nitrogen pressure (0.1 MPa). However, thermodynamic calculation of the reaction (1) performed in Ref.[13] indicates that at 0.1 MPa, the Gibbs free energy change ΔG° is negative at temperatures below 1715 °C. This calculation shows that the reaction (1) may proceed towards the right-hand side and form Mo_5Si_3 and Si_3N_4. Note that in both sintering atmospheres no crystalline grain boundary phases were observed as shown in Fig. 2.

SEM micrographs of the polished and etched compact materials consolidated in nitrogen atmosphere are shown in Fig. 3. The compacts had a two-phase structure. The brighter areas correspond to $MoSi_2$ (or Mo_5Si_3) grains and the darker grains are Si_3N_4. The grain sizes for $MoSi_2$/Mo_5Si_3 are summarized in Table 2.

It can be seen that in the SM1 (Fig. 3a) and SM3 (Fig. 3c) composites the $MoSi_2$/Mo_5Si_3 grains have an irregular shape and are homogeneously distributed in the Si_3N_4 matrix. In these

Table 2
$MoSi_2$/Mo_5Si_3 grain size and phase composition of materials obtained.

Number	Phase composition		Grain size of $MoSi_2$/Mo_5Si_3 (μm)	
	In nitrogen	In argon	In nitrogen	In argon
SM1	$MoSi_2$, β-Si_3N_4, traces of Mo_5Si_3	–	2–4	–
SM2	$MoSi_2$, β-Si_3N_4, Mo_5Si_3	–	3–4	–
SM3	$MoSi_2$, β-Si_3N_4, Mo_5Si_3	–	3–4	–
SM4	$MoSi_2$, β-Si_3N_4, traces of Mo_5Si_3	–	0.5–4	–
SM5	$MoSi_2$, β-Si_3N_4, Mo_5Si_3	$MoSi_2$, β-Si_3N_4	0.5–2	0.5–2
SM6	$MoSi_2$, β-Si_3N_4, Mo_5Si_3	$MoSi_2$, β-Si_3N_4	0.5–2	0.5–2

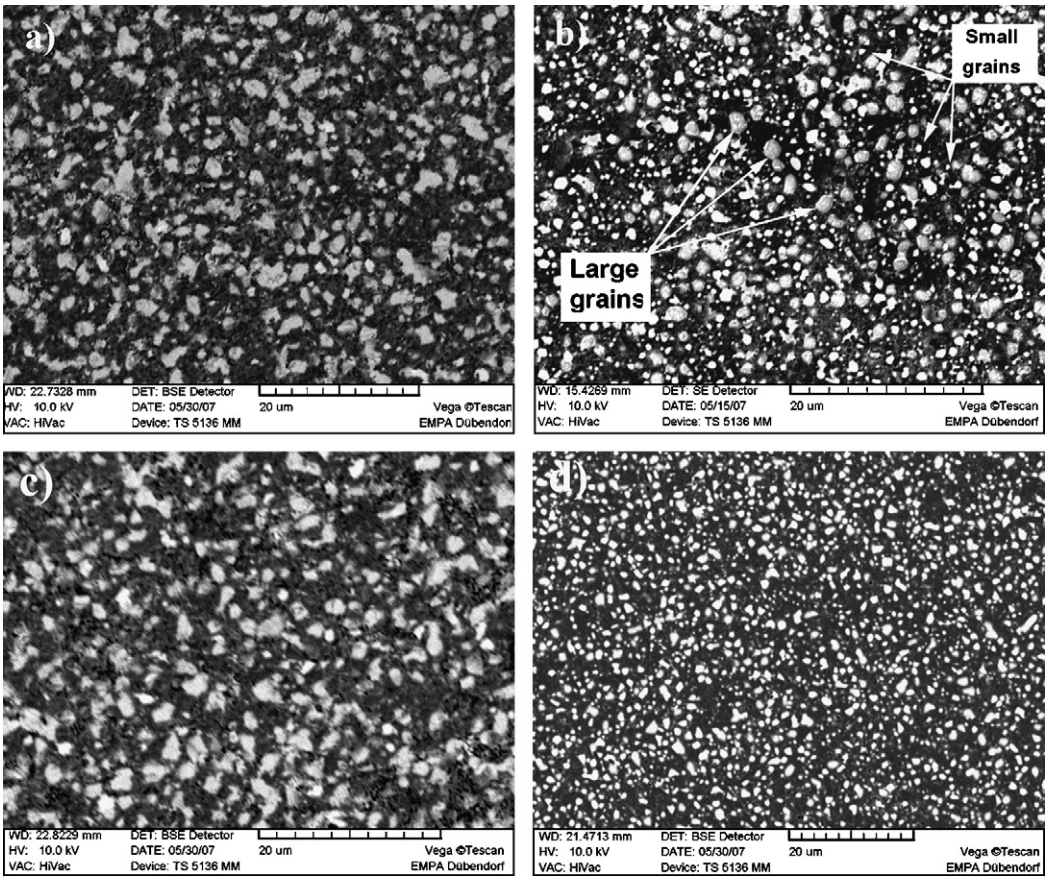

Fig. 3. Microstructure of compact samples: (a) SM1, (b) SM4, (c) SM3, (d) SM5 compacted in nitrogen atmosphere.

compacts, silicide grains have relatively large particle sizes (3–4 μm). In the SM4 compacts (Fig. 3b), two types of $MoSi_2$ grains were observed: (i) large particles with 2–4 μm in size and (ii) grains below 1.5 μm. These grains also have different shapes. Smaller grains are spherical, while larger ones are irregular shaped. It is assumed that the small grains are particles of combustion synthesized $MoSi_2$ powder. This assumption was confirmed by the fact that composites fabricated from commercial Si_3N_4 and only SHS-$MoSi_2$ powders contain spherical grains (Fig. 3d) with sizes typically smaller than 2 μm.

The sintering atmosphere has a significant influence on the microstructure of dense composites. It was observed that composites SM5 and SM6 sintered in a nitrogen environment led to the formation of dense samples (Fig. 4a), with the β-Si_3N_4 rod-like grains having a width of ∼1 μm and a length of up to 5 μm. The same composite sintered in the Ar atmosphere contains equiaxed shaped grains of the β-Si_3N_4 (Fig. 4b).

3.2. Electrical properties

The control of the microstructure of such composite materials can lead to adjustable electrical properties. It is well-known that the mechanism of the electrical conduction for such composite materials is the formation of a percolating network of the electrical conductive phase within the Si_3N_4 matrix, the distribution of conductive particles is one of the most important factors influencing the electrical conductivity. It was shown in Refs.[13,23] that electrical conductivity of $MoSi_2$–Si_3N_4 composite materials depends on $MoSi_2$ concentration. In particular, the electrical conductivity of the materials increased with $MoSi_2$ volume fraction in a manner typical for percolation systems. At low $MoSi_2$ concentrations, the isolated $MoSi_2$ particles were dispersed in the insulating Si_3N_4 matrix and hence the electrical conductivity was very low. A strong increase in conductivity was observed when the $MoSi_2$ concentration reached the critical value (approximately 20–30 vol.%), when the distribution state of the electroconductive particles changed from a dispersive distribution to a continuous network distribution.[8,13]

In this research, the electrical conductivity of materials sintered in nitrogen atmosphere was measured at room temperature (Table 3). It was expected from the above discussion that the SM1 composite with 22 vol.% of the conductive phase would be

Table 3
Room temperature electrical conductivity for composites sintered in nitrogen.

Number	Conductivity (Ω^{-1} cm^{-1})
SM1	1.1×10^{-10}
SM2	4.3×10^{-7}
SM3	9.7×10^{-6}
SM4	6.2×10^{2}
SM5	8.3×10^{-8}
SM6	5.4×10^{-5}

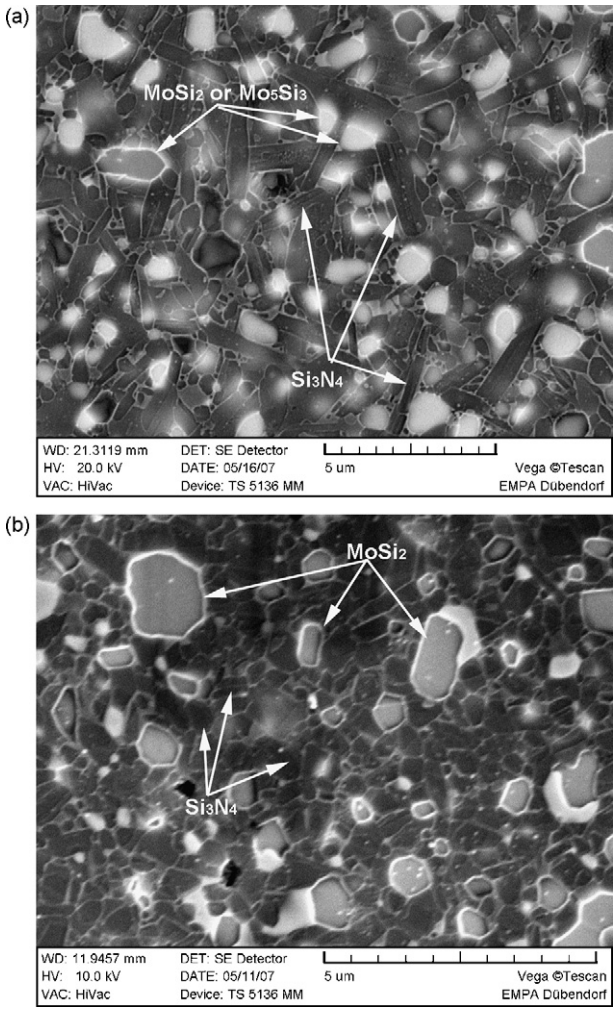

Fig. 4. Microstructure of 40% $MoSi_2$–Si_3N_4 (SM6) composite compacted in N_2 (a) and Ar (b) atmospheres.

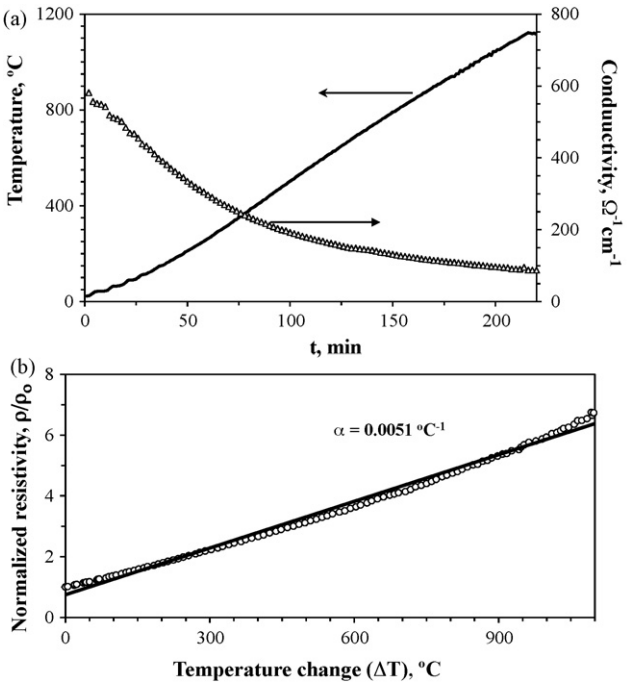

Fig. 5. Double plot of temperature and electrical conductivity vs. time for the SM4 composite (a) and plot of normalized electrical resistivity (ρ/ρ_o) vs. temperature (b).

an insulator. Actually, the electrical conductivity of SM1 sintered at 1700 °C was measured to be very low ($\sim 10^{-10}\,\Omega^{-1}\,cm^{-1}$) which is close to values typical for insulators.[24] In contrast with this result room temperature conductivity of SM4 materials was $\sim 6 \times 10^2\,\Omega^{-1}\,cm^{-1}$. Note that according to results of XRD analysis, apart from SM4 composite other materials consolidated in the nitrogen atmosphere contain certain amount of Mo_5Si_3. The Mo_5Si_3 is also an electrical conductor ($\sim 10^5\,\Omega^{-1}\,cm^{-1}$). However, taking in to account reaction (1) and the molar volumes of $MoSi_2$ ($24.4\,cm^3\,mol^{-1}$) and Mo_5Si_3 ($68.3\,cm^3\,mol^{-1}$) one can conclude that in the case of full nitridation of $MoSi_2$ that a sharp decrease in volume takes place (about 1.8 times). Moreover, in the case of full nitriding of $MoSi_2$–Si_3N_4 composites containing 30 or 40 vol.% of $MoSi_2$ leads to reduction of volume fraction of conductive phase (Mo_5Si_3) down to 15 or 20 vol.%, respectively. From the results of XRD analyses for samples SM2, SM3, SM5 and SM6 significant amount of $MoSi_2$ transformed in to the Mo_5Si_3 and Si_3N_4. As a result the electrical conductivity of compacts for SM2, SM3, SM5 and SM6 was measured to be in the range 10^{-8} to $10^{-5}\,\Omega^{-1}\,cm^{-1}$.

Other important factors influencing the conductivity of such composites are the particle size of the conductive phase and the ratio between the diameter of insulating and conductive particles. It was shown[8] that $MoSi_2$–Si_3N_4 composites containing 30 wt.% (~23–24 vol.%) $MoSi_2$ changed from a conductor to an insulator by decreasing the diameter ratio of Si_3N_4 to $MoSi_2$ particles from 10:1 to 3:1. In our case, homogenously distributed small grains (below 1.5 μm) of $MoSi_2$ phase in the SM4 compact samples (see Fig. 3b) contribute to the formation of a good conductive composite.

High temperature application of such conductive composites must be validated by studying their electrical properties at elevated temperatures. The conductivity of SM4 material was measured up to 1100 °C (Fig. 5a). The results obtained have shown that this composite exhibits positive temperature coefficient of resistivity over the whole temperature range. This indicates that metallic-like electron conduction is the dominant conduction mechanism. Therefore, electrons are transported mainly through the conductive $MoSi_2$ percolating paths. The temperature coefficient of resistivity (α) is one of the most important characteristic parameters for a conductor and it can be calculated according to the following equation:

$$\frac{\rho}{\rho_o} = 1 + \alpha \Delta T$$

where ρ is the electrical resistivity at a given temperature; ρ_o is the electrical resistivity at room temperature; ΔT is equal to $T - T_o$. The α value of the SM4 composite was obtained from the slope of the ρ/ρ_o against ΔT plot (Fig. 5b). The small deviation of the data points from a straight line may be due to the error

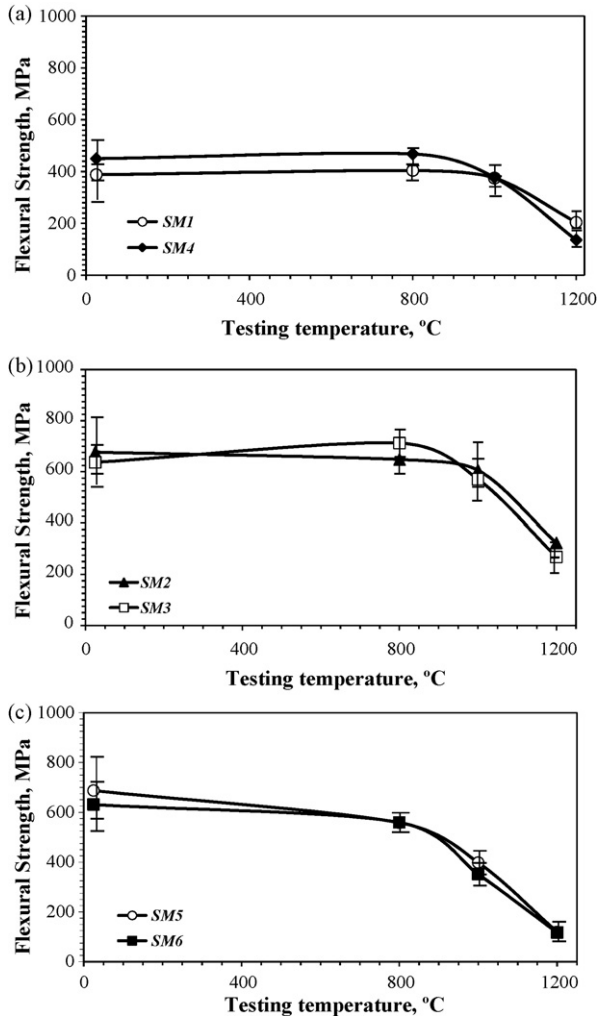

Fig. 6. The flexural strength of the composites as a function of temperature, for SM1 and SM4 materials (a), for SM2 and SM3 (b), and for SM5 and SM6 (c) error bars represent the standard deviations of 3–4 tests at each temperature.

induced by the surface oxidation during the measurements at high temperatures.

3.3. Mechanical properties

The flexural strengths of all six materials sintered in a nitrogen atmosphere as a function of temperature are presented in Fig. 6. At room temperature, the strength for SM1 and SM4 composites was 388 and 450 MPa, respectively. The values obtained are the average of 3–4 bend tests performed per material. It can be seen that the flexural strength for the relatively fine-phase material (SM4) was quite high (Fig. 6a). The strength remained stable between room temperature and 800 °C. The flexural strength for both composites degraded significantly when the temperature was raised above 800 °C. The strength of the SM1 composite was 374 and 205 MPa at 1000 and 1200 °C, respectively. However, at 1200 °C the SM1 material was stronger than the SM4 one. In particular, the strengths of the SM1 and SM4 composites were 205 and 136 MPa, respectively. In contrast to SM1 and SM4 materials, the composites fabricated only from commercial powders demonstrated higher values of flexural strength. At room temperature, the strength was 676 and 636 MPa for SM2 and SM3 composites, respectively. The strength up to about 800 °C did not change for both composites. At 1200 °C the flexural strength for the SM2 and SM3 composites was 323 and 268 MPa, respectively. For the next two composite materials, SM5 and SM6, the room temperature strength was close to the materials fabricated from commercial powders, changing between 631 and 687 MPa. Fig. 6c shows that the high temperature flexural strength of SM5 and SM6 composites start to decrease significantly at around 800 °C. At 1200 °C the strength of these two materials showed the lowest values (~120 MPa) of all tested composites.

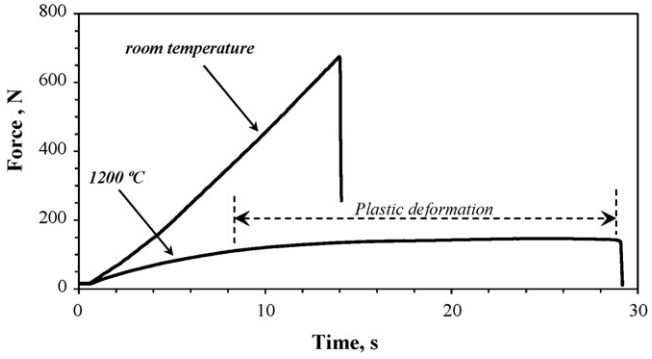

Fig. 7. Bending profiles of SM5 composite at room and elevated temperatures.

It was proposed in Ref.[5] that two deformation mechanisms lead to fracture of $MoSi_2$–Si_3N_4 composites at high temperatures:

(i) grain boundary sliding; and
(ii) dislocation glide/climb in the $MoSi_2$ phase.

On the other hand, it was shown in Ref.[14] that the contribution of grain boundary sliding to deformation in final fracture is negligible. It is well-known that the brittle–ductile transition temperature of $MoSi_2$ is around 1000 °C,[25] above which dislocation glide is activated. Therefore, the plastic deformation of $MoSi_2$ may have a major contribution to the sharp strength degradation of $MoSi_2$–Si_3N_4 composites at high temperatures. In our research the contribution of plastic deformation was confirmed by the character of the force vs. time curves at room and elevated temperatures (Fig. 7). Although it is not possible to rule out that some sub-critical crack growth (SCG) or microcracking may have occurred it was not detectable by fractography. SCG or microcracking can be detected in ceramics by the careful observation for "halos" around the fracture origin.[26] In addition, covalently bonded ceramics (e.g. Si_3N_4) are normally not susceptible to SCG.[26]

The fracture toughness (K_{Ic}) of all composites sintered in nitrogen atmosphere was measured by the SEVNB method. The error associated with each fracture measurement by SEVNB measurements was typically ±5%. The room temperature fracture toughness of the tested composites was in the range from 3.7 to 5.5 MPa $m^{1/2}$, which is generally close to the range reported for monolithic Si_3N_4 ~4.3–5.4 MPa $m^{1/2}$.[27] The K_{Ic} is in gen-

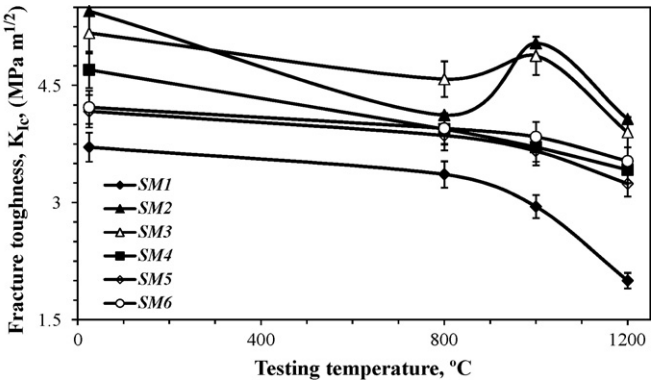

Fig. 8. The average values of fracture toughness of composite materials vs. temperature.

eral dependent on the microstructural features of the Si_3N_4. A high K_{Ic} is normally associated with elongated β-Si_3N_4 grains, in the current work this type of microstructure is not relevant except in SM6 when sintered under N_2. Room temperature toughness increased from 3.7 to 4.7 MPa m$^{1/2}$ for the SM1 and SM4 composites when $MoSi_2$ concentration was increased from 22 to 30 vol.%. These results comply with the results obtained in Ref.[5] that at room temperature K_{Ic} value increases with increasing concentration of $MoSi_2$ in the composite. In the two composites, SM2 and SM3, the opposite result was observed; increasing the $MoSi_2$/Mo_5Si_3 concentration from 30 to 40 vol.% resulted in a small decrease in the fracture toughness from 5.4 to 5.2 MPa m$^{1/2}$. The results are consistent with literature which report an increase of K_{Ic} with the introduction of $MoSi_2$ into Si_3N_4 matrixes due to toughening mechanisms including residual stresses and crack deflection.[28] However, at a certain level there is then a decrease in the K_{Ic} when an excess of $MoSi_2$ is added, work by others indicate that this is at approximately 37 vol.% $MoSi_2$ content.[29]

In the composites SM5 and SM6 room temperature fracture toughness practically is the same. Summarizing the results obtained for room temperature measurements, it may be concluded that fine-grained $MoSi_2$/Mo_5Si_3 containing composites (SM4, SM5 and SM6) showed only a modest fracture toughness, while the coarse-grained $MoSi_2$/Mo_5Si_3–Si_3N_4 composites (SM2 and SM3) exhibited higher fracture toughness, reaching higher values than 5 MPa m$^{1/2}$. As for the SM1 composite, it displayed the lowest K_{Ic} value.

Fracture toughness of all six materials sintered in a nitrogen atmosphere was also measured at 800, 1000, and 1200 °C (Fig. 8). It was shown that the temperature dependencies of K_{Ic} for SM4, SM5, and SM6 have similar characteristics. The fracture toughness of these composites decreased from about 4 MPa m$^{1/2}$ to about 3.4 MPa m$^{1/2}$ with the temperature increasing from 800 to 1200 °C. The small difference in K_{Ic} values measured for SM4, SM5, and SM6 can be explained by the influence of the relatively small $MoSi_2$/Mo_5Si_3 grains formed from SHS-$MoSi_2$ powder. From this viewpoint, it was expected that SM1 would exhibit high fracture toughness, however, the fracture toughness of SM1 was the lowest of all composites. Moreover, fracture toughness of this composite at 1200 °C was very low (2 MPa m$^{1/2}$). The fracture toughness of SM1 is lowest because it had the lowest amount of $MoSi_2$ content. It has small equiaxed $MoSi_2$ and Si_3N_4 grains, this grain morphology leads to lower mechanical properties at high temperature compared to the composites with elongated Si_3N_4 grains, e.g. SM6.

The other two composites (SM2 and SM3), which were fabricated from commercially available starting powders, exhibited a high fracture toughness. The K_{Ic} value of these materials was 4.3 and 4.7 MPa m$^{1/2}$ for SM2 and SM3 at 800 °C, respectively. At 1000 °C a local maximum (∼5 MPa m$^{1/2}$) was measured for these materials. The reason for this maximum is unclear, yet, but might be related to a softening of the glassy phase at the grain boundary. A steep decrease in fracture toughness was observed at 1200 °C, where the K_{Ic} was approximately 4 MPa m$^{1/2}$ for both materials.

4. Conclusions

$MoSi_2$–Si_3N_4 and $MoSi_2$–Mo_5Si_3–Si_3N_4 composites from commercially available individual compounds, one-stage combustion synthesized $MoSi_2$–Si_3N_4 and SHS $MoSi_2$ powders were produced by hot pressing in nitrogen and argon atmospheres. The phase composition, microstructure, electrical and mechanical properties were studied and the following results were obtained:

- During hot pressing the $MoSi_2$ phase was partly nitrided by nitrogen to form Mo_5Si_3. The nitridation of $MoSi_2$ could be prevented by using Ar atmosphere. The microstructure of the components mainly depends on the particle size of the starting powders and the sintering atmosphere. Composites sintered in a nitrogen atmosphere were dense with rod-like Si_3N_4 grains, but when sintered in an Ar atmosphere the silicon nitride grains had an equiaxed shape.
- The room temperature electrical conductivity of the $MoSi_2$–Si_3N_4 composite sintered in nitrogen was measured. The composite with 30 vol.% of $MoSi_2$ exhibited positive temperature coefficient of resistivity and a metallic-like conduction was the dominant conduction mechanism.
- The flexural strength of the composites fabricated from SHS $MoSi_2$ powder and commercial Si_3N_4 powder was high at room temperature: 650–680 MPa. In all composites the strength decreased significantly at temperatures above 1000 °C due to the brittle–ductile transition of the $MoSi_2$ phase. From all composites only materials fabricated from commercial powders exhibited a room temperature fracture toughness higher than 5 MPa m$^{1/2}$. At elevated temperatures the SM2 and SM3 composites exhibited a low fracture toughness of about 4–4.5 MPa m$^{1/2}$.

Acknowledgements

The authors would like to thank for the support by the Swiss National Science Foundation (Project no. PIOI2-117177). The authors are grateful to Mr. Roland Baechtold for his assistance in the mechanical testing of materials.

References

1. Petrovic, J. J. and Honnell, R. E., $MoSi_2$ particle reinforced-SiC and Si_3N_4 matrix composites. *J. Mater. Sci. Lett.*, 1990, **9**, 1083–1084.
2. Kao, M. Y., Properties of silicon nitride–molybdenum disilicide particulate ceramic composites. *J. Am. Ceram. Soc.*, 1993, **76**, 2879–2883.
3. Petrovic, J. J., Pena, M. I. and Kung, H. H., Fabrication and microstructures of $MoSi_2$ reinforced-Si_3N_4 matrix composites. *J. Am. Ceram. Soc.*, 1997, **80**, 1111–1116.
4. Zhang, B. R. and Marino, F., Reaction-bonding preparation of Si_3N_4/$MoSi_2$ and Si_3N_4/WSi_2 composites from elemental powders. *J. Am. Ceram. Soc.*, 1997, **80**, 269–272.
5. Petrovic, J. J., Pena, M. I., Reimanis, I. E., Sandlin, M. S., Conzone, S. D., Kung, H. H. *et al.*, Mechanical behavior of $MoSi_2$ reinforced-Si_3N_4 matrix composites. *J. Am. Ceram. Soc.*, 1997, **80**, 3070–3076.
6. Kowalik, R. W. and Hebsur, M. G., Cyclic oxidation study of $MoSi_2$–Si_3N_4 base composites. *Mater. Sci. Eng.*, 1999, **A261**, 300–303.
7. Alman, D. E., Tylczak, J. H., Hawk, J. A. and Hebsur, M. G., Solid particle erosion behavior of an Si_3N_4–$MoSi_2$ composite at room and elevated temperatures. *Mater. Sci. Eng.*, 1999, **A261**, 245–251.
8. Yamada, K. and Kamiya, N., High temperature mechanical properties of Si_3N_4–$MoSi_2$ and Si_3N_4–SiC composites with network structures of second phases. *Mater. Sci. Eng.*, 1999, **A261**, 270–277.
9. Klemm, H. and Schubert, C., Silicon nitride/molybdenum disilicide composite with superior long-term oxidation resistance at 1500 °C. *J. Am. Ceram. Soc.*, 2001, **84**, 2430–2432.
10. Beruto, D. T., Ferrari, A., Giordani, M. and Marino, F., Kinetic mechanism and microstructure during the formation of Si_3N_4 matrix in Si_3N_4–$MoSi_2$ composites. *Mater. Sci. Eng.*, 2003, **A355**, 286–291.
11. Singh, S., Godkhindi, M. M., Krishnarao, R. V. and Murty, B. S., Synthesis of Si_3N_4–$MoSi_2$ in situ composite from mechanically activated (Mo + Si_3N_4) powders. *J. Alloys Compd.*, 2004, **381**, 254–257.
12. Wang, G., Jiang, W., Bai, G. and Chen, D., Si_3N_4 rodlike crystal-reinforced $MoSi_2$ matrix composites. *Mater. Lett.*, 2004, **58**, 308–311.
13. Guo, Zh., Blugan, G., Graule, G. T., Reece, M. and Kuebler, J., The effect of different sintering additives on the electrical and oxidation properties of Si_3N_4–$MoSi_2$ composites. *J. Eur. Ceram. Soc.*, 2007, **27**, 2153–2161.
14. Guo, Zh., Parlinska-Wojtan, M., Blugan, G., Graule, T., Reece, M. and Kuebler, J., The influence of the grain boundary phase on the mechanical properties of Si_3N_4–$MoSi_2$ composites. *Acta Mater.*, 2007, **55**, 2875–2884.
15. Petrovic, J. J. and Vasudevan, A. K., Key developments in high temperature structural silicides. *Mater. Sci. Eng.*, 1999, **A261**, 1–5.
16. Schneibel, J. H. and Sekhar, J. A., Microstructure and properties of $MoSi_2$–MoB and $MoSi_2$–Mo_5Si_3 molybdenum silicides. *Mater. Sci. Eng.*, 2003, **A340**, 04–211.
17. Liu, Y. Q., Shao, G. and Tsakiropoulos, P., On the oxidation behaviour of $MoSi_2$. *Intermetallics*, 2001, **9**, 125–136.
18. Liu, C. C., Microstructure and tool electrode erosion in EDMed of TiN/Si_3N_4 composites. *Mater. Sci. Eng.*, 2003, **A363**, 221–227.
19. Manukyan, Kh. V., Aydinyan, S. V., Kirakosyan, Kh. G., Kharatyan, S. L., Blugan, G., Müller, U. *et al.*, Salt-assisted combustion synthesis and characterization of $MoSi_2$ and $MoSi_2$–Si_3N_4 composite powders. *Chem. Eng. J.*, 2008, **143**, 331–336.
20. CEN 843-1, Advanced Technical Ceramics – Monolithic Ceramics – Mechanical Properties at Room Temperature – Part 1: Determination of Flexural Strength, 1995.
21. CEN/TS 14425-5, Advanced Technical Ceramics – Test Methods for Determination of Fracture Toughness of Monolithic Ceramics – Part 5: Single-Edge V-Notch Beam (SEVNB) Method, 2004.
22. ASTM F43–93, Standard test methods for resistivity of semiconductor materials, *Annual Book of ASTM Standards*, 1993, **10.5**, 33–38.
23. Sciti, D., Guicciardi, S. and Bellosi, A., Microstructure and properties of Si_3N_4–$MoSi_2$ composites. *J. Ceram. Proc. Res.*, 2002, **3**, 87–95.
24. Ashby, M., Shercliff, H. and Cebon, D., *Materials: Engineering, Science, Processing and Design*. Elsevier, Oxford, 2007, pp. 311–342.
25. Vasudeĭnvan, A. K. and Petrovic, J. J., A comparative overview of molybdenum disilicide composites. *Mater. Sci. Eng.*, 1992, **A155**, 1–17.
26. Quinn, G. D., Fractography of Ceramics and Glasses, NIST recommended practice guide, 2007, SP, 960-16.
27. Kübler, J., Fracture toughness of ceramics using the SEVNB method: preliminary results. In *Ceramic Engineering and Science Proceedings*, *vol. 18*, ed. J. P. Singh. American Ceramic Society, 1997, pp. 155–162.
28. Sciti, D., Celotti, G. C., Pezzetti, G. and Guicciardi, S., Effect of $MoSi_2$ particles on the fracture toughness of AlN-, SiC, and Si_3N_4-based ceramics. *J. Compos. Mater.*, 2007, **14**, 2585–2593.
29. Krishnarao, R.V., Kumari, S., Srinivasarao, M. and Subrahmanyam, J., Development of $MoSi_2$–Si_3N_4 insitu composites by reaction of molybdenum with silicon nitride, Processing and Fabrication of Advanced Materials XIV with Frontiers in Materials Science 2005: Innovative Materials and Manufacturing Techniques, Proceedings, pp. 501–516.